

山东理工大学

SHANDONG

/

_____

_____

_____

20120803116

_____

2024 6

α-

DMSO CMOM CMNM

CMNM CMOM

CMOM CMNM

HOMO LUMO CMNM HOMO

LUMO HOMO

CMOM

CMOM CMNM

CMOM CMNM

Abstract

Coumarin is a benzopyranone produced by the fusion of a benzene ring and a α-pyrone ring. The application of coumarin is mainly by introducing substituents at different positions of coumarin to adjust its optical and chemical properties to achieve cell imaging, environmental monitoring and other applications. The absorption spectrum of coumarin dye is in the ultraviolet to blue region, and the emission spectrum is in the blue to green region. Coumarin fluorescent dyes have a high fluorescence quantum yield and can effectively convert the absorbed light energy into fluorescence. At the same time, the excellent photostability of coumarin fluorescent dyes is suitable for long-term light experiments. At the same time, the addition of a modified group to the coumarin group can change the solubility, polarity and optical properties of the dye. For example, the introduction of a morpholine group on the coumarin group can increase the solubility of coumarin-based fluorescent dyes, which can increase the biocompatibility of the fluorescent dye. Coumarin fluorescent dyes have been widely used in bioimaging, fluorescent probes, optoelectronic materials and other fields due to their diverse chemical modification possibilities and excellent optical properties. Future research will continue to explore its potential for broader applications, particularly to further optimize its performance through molecular design.

Firstly, the dihedral angles of CMOM and CMNM were analyzed under dimethyl sulfoxide (DMSO) solvent, and it was concluded that the bond angle changes of CMNM and CMOM were similar, the dihedral angle between piperazine and coumarin changed the least, and the dihedral angle between methylenemalononitrile and coumarin changed the most, and it was concluded that morpholine and piperidine had an effect on their respective molecules, but the magnitude of the influence was not large.

Then, the absorption and emission wavelengths of CMOM and CMNM were obtained through experimental calculations, and the oscillator intensity and transition component ratio of the two molecules were calculated, and it was found that the HOMO and LUMO diagrams of the two molecules were quite different, and the HOMO of the

molecule CMNM was almost evenly distributed in the part except the piperazine group, while the LUMO was offset to the malononitrile methylene modified group on the basis of HOMO, while the electron cloud distribution on the other side was less or even none. The situation is similar for CMOM.

Finally, the reforming energies and radiation-free spectral lines of CMOM and CMNM in solution were calculated, and the dissipation pathways of the molecules were compared. The radiative and non-radiative transition rates of CMOM and CMNM in solution were calculated, and the reasons for the different results of the two molecules were analyzed.

Key words: Coumarin, electron cloud density, recombination energy, radiative and non radiative processes

.....I

ABSTRACT.....II

1 1

1.1 1

1.1.1 2

1.1.2 3

1.1.3 5

1.2 6

1.2.1 6

1.2.2 7

1.2.3 7

1.3 8

1.3.1 8

1.3.2 9

1.4 9

2 11

2.1 11

2.1.1 11

2.1.2 12

2.2 PCM 13

2.3 14

2.3.1 Joblonski 14

2.3.2 15

2.3.3 17

2.4 18

3 19

3.1 19

3.2 20

3.3 22

3.4 27

.....30

.....31

.....35

Rhodamine Fluorescein Coumarin

OLED

1

1.1

Rhodamine

Fluorescein Coumarin

OLED

[1]

π-

[2]

1-1 4 5

-

1.1.1

1-1 4 5

-



萘酰亚胺

1-1

[[3],[4] 1 8-

[5]

[6],[7] 1 8-

[8]

4

4

[9],[10] DSSC Lin DSSC

DSSC 10.8% N719 [11]

[[3],[4] 1 8-

[5]

[6],[7] 1 8-

[8]

4 4

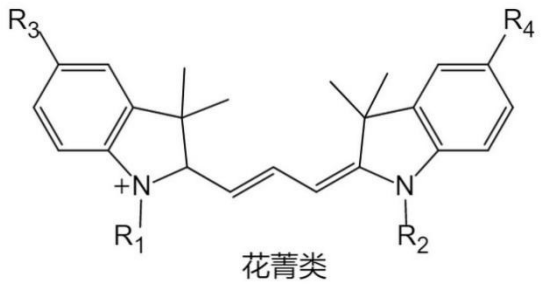
[9],[10]

DSSC Lin DSSC

DSSC 10.8% N719 [11]

1.1.2

1-2



花菁类

1-2

[12]

[12]

[13] [14]

[15],[16]

; 2006 Chipon

DNA [17]

[18]

N

---

[13]

[14]

[15],[16] ;

2006 Chipon

DNA [17]

[18]

N

0.06-0.4 ps ns [17]

C-C [18] [19]

-

[20] [21]

Sanborn Cy3 DNA [22]

1.1.3

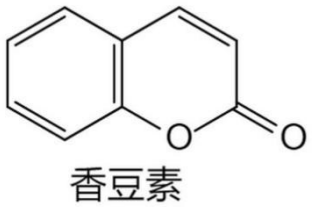
1-3 α-

1-3 α-

OLED NLO

HIV

OLED NLO HIV



香豆素

1-3

3- 7- $\lambda_{max,abs}$ =330 nm; $\lambda_{max,emi}$=380 nm Φ_F [23] π-

- D-A ICT [24],[25] Con

i ii

iii iv [26],[27] [g/f/h]

i

ii iii iv [26],[27]

[g/f/h] π-

[28]

pi [29]

[30],[31]

---

[28]

pi

[29]

[30],[31]

1.2

1.2.1

Zhang L- - -

HeLa

HeLa [32]

1.2.2

pH

Zhang ICT

pH pH BODIPY 3 5- BODIPY

pH Zhang

ICT pH pH

BODIPY 3 5- BODIPY

pH BODIPY

BODIPY pH pH

BODPY pH

[33]

---

pH BODIPY BODIPY

pH pH

BODPY

pH

[33]

1.2.3

-

1.3

Cys Cys

Cys Cys

0.06 μM

[34]

[35]

1.3.1

N_2H_4

λ_{ex}=390 nm λ_{em}=650/450 nm

N2H4

λex=390 nm

λem=650/450 nm (F450/F650)

(2.05–996 μM) (pH 5–11) 20

2 min Sa-Sa Zhu -

pH [36] pH

(F_{450}/F_{650}) (2.05–996 μM) (pH 5–11)

20 2 min

Sa-Sa Zhu - pH [36]

pH

SO_2

(IL) SO_2 IL

SO_2 IL SO_2 <0.2 ppm

>12 SO_2

1.3.2

(LD)

/

1,3- / [4,3-*b*] [3,4-*d*] 4-4 3*H*

NH_4 OAc/ NMR X

chromeno [4,3-*b*] [3,4-*d*] pyridin-4 3*H*

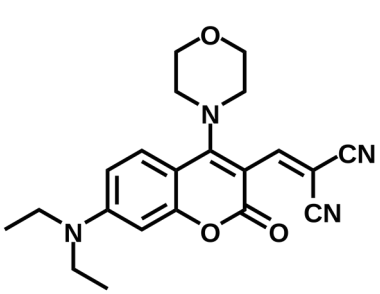
Φ_F 0.53

1.4

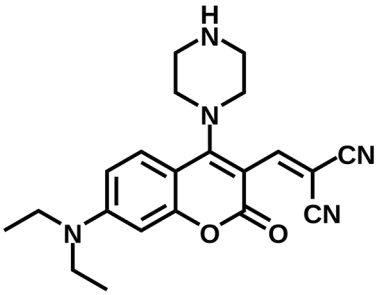
PCM

PCM

DMSO



CMOM



CMNM

1-4 CMOM CMNM

(DFT)

2

2.1

2.1.1

(DFT)

(1) Thomas-Fermi

Thomas-Fermi Llewellyn Thomas Enrico Fermi 1920

$$E_{TF}\left[\rho(r)\right] = C\int\rho^{5/3}(r)dr - z\int\frac{\rho(r)}{r}dr + \frac{1}{2}\iint\frac{\rho(r_1)\rho(r_1)}{\left|r_1 - r_1\right|}dr_1dr_2 \qquad 2\text{-}1$$

2 Hohenberg-Kohn

Hohenberg-Kohn Density Functional Theory, DFT 1964 Pierre Hohenberg Walter Kohn Hohenberg-Kohn

Hohenberg-Kohn

$$\psi = \psi\left(\rho(r_1, r_2, r_3 \cdots r_1)\right) \qquad 2\text{-}2$$

Hohenberg-Kohn

3 Kohn-Sham K-S

Walter Kohn Lu Jeu Sham 1965 Kohn-Sham

$$\hat{H}_{KS}\psi_i \equiv \left[-\frac{1}{2}\nabla^2 + V_{eff}(\vec{r}) \right] \psi_i(r) = \varepsilon_i \psi_i(r) \qquad 2\text{-}3$$

2.1.2

TD-DFT

K-S

$$i\frac{\partial \phi_j(r,t)}{\partial t} = \left\{ -\frac{\nabla^2}{2} + v_{KS}[n](r,t) \right\} \phi_j(r,t) \qquad 2\text{-}4$$

$[n](r,t)$

$$[n](r,t) = \sum_{j=1}^{N} |\phi_j(r,t)|^2 \qquad 2\text{-}5$$

KS $v_{KS}[n](r,t)$

$$v_{KS}[n](r,t) = v_{ext}(r,t) + v_H(r,t) + v_{XC}(r,t) \qquad 2\text{-}6$$

Hartree $v_H(r,t)$

$$v_H(r,t) = \int d^3r' \frac{n(r',r)}{|r - r'|} \qquad 2\text{-}7$$

TD-DFT

$$n(r,t) = n_{GS}(r,t) + \delta n(r,t) \qquad 2\text{-}8$$

$n_{GS}(r,t)$ $\delta n(r,t)$

$$v_{XC}[n_{GS} + \delta n](r,t) = v_{XC}[n_{GS} + \delta n](r) + \int dt' \int d^3r' f_{XC}[n_{GS}](r,r',t - t')\delta n(r',t')$$

2-9

f_{XC} TD-DFT

$$\int d^3r' f_{XC}[n_{GS}](r,r',t - t') = \frac{\delta v_{XC}(r,t)}{\delta n(r',t')} \qquad 2\text{-}10$$

Dyson

$$\xi(r,r',\omega)=\xi_{KS}(r,r',\omega)+\int d^3r_1\int d^3r_2\xi_{KS}(r,r',\omega)\left\{\frac{1}{|r_1-r_2|}+f_{XC}(r,r',\omega)\right\}\xi(r_2,r',\omega)$$

2-11

Gaussian16 E_{vert}

2.2 PCM

1981 PCM

[38] PCM

DMSO

CMOM CMNM -

-

CMOM CMNM DMSO

PCM

PCM LR

CMOM CMNM

TD-

DFT LR

DMSO CMOM CMNM PCM

IE

LR

CMOM CMNM Gaussian 16

CMOM CMNM 2-1 CMOM CMNM PCM

Joblonski

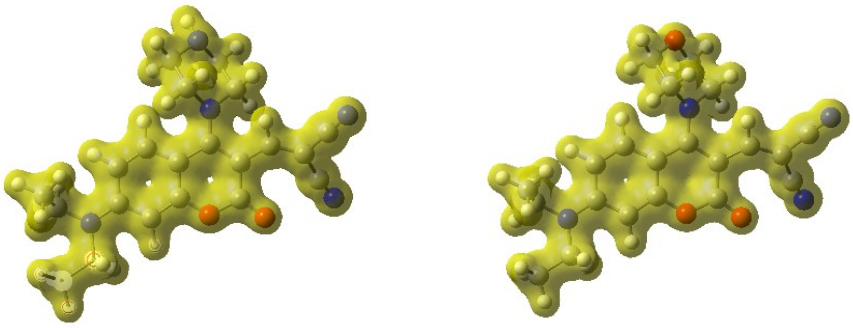
S0 S1

[39] Stokes

ISC [40]

S1 S0

Stokes



2-1 CMOM CMNM PCM

2.2

2.2.1 Joblonski

Joblonski

S_0

S_1

[39]

Stokes

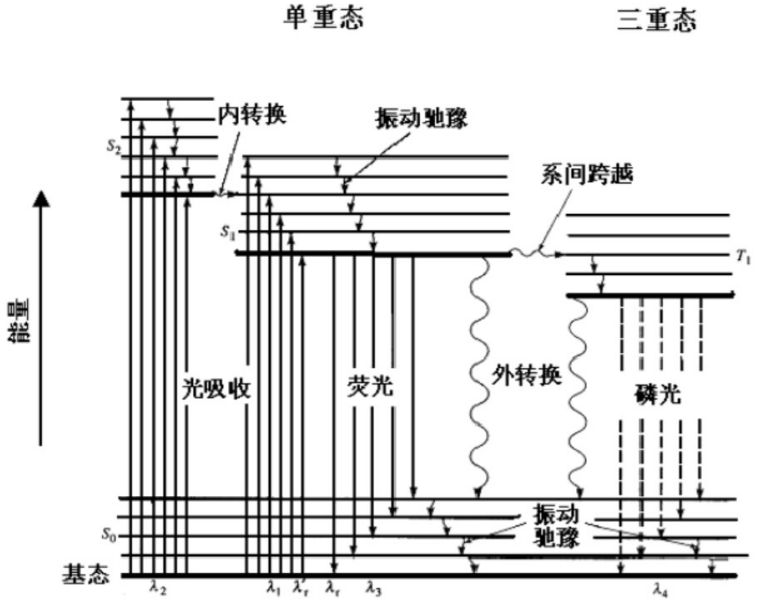
ISC [40] S1

S0

Stokes

Joblonski CMOM CMNM

[41]



2-2 Jablonski

2.2.2

Joblonski

CMOM CMNM k_r [41]

$$k_r = \frac{f E_{vert}^2}{1.499\ s \cdot cm^{-2}}$$

2-18

f E_{vert} cm^{-1} k_r s^{-1}

k_{ic}

k_{ic}

$$k_{ic} = \sum_{kl} \frac{1}{\hbar^2} R_{kl} \int_{\infty}^{\infty} dt \left[e^{i\omega_{if} t} Z_i^{-1} \rho_{IC}(t,T) \right] \quad 2\text{-}19$$

HR

$$HR_j = \frac{D_j^2 \omega_j}{2\hbar} \quad 2\text{-}20$$

D_j S_0 S_1 j MOMAP

S_j

$$\lambda_{g(e)} = \sum_{j \in g(e)} \lambda_j = \sum_{j \in g(e)} \hbar S_j \omega_j \quad 2\text{-}21$$

2.2.3

ISC

S_1 S_0 T_1 S_0 ISC

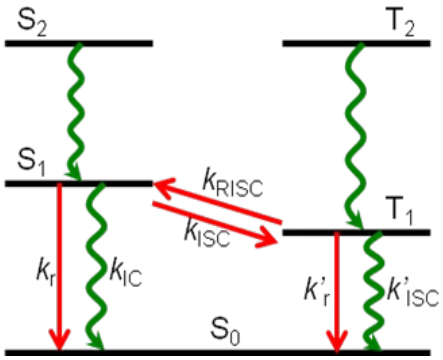
IC S_2 S_1 VR

Φ_F Φ_F

$$\Phi_F = \frac{k_r}{k_r + k_{nr}} = \frac{k_r}{k_r + k_{ic} + k_{isc}} \quad 2\text{-}20$$

k_{ISC} Φ_F

$$\Phi_F = \frac{k_r}{k_r + k_{ic}}$$ 2-21



2-3

pH

pH pH

Φ_F Error: Reference source not found

2.3

GaussView CMOM CMNM

Linux B3LYP 6-31G(d)

Gaussian 16

PCM

S_1 DFT TD-DFT

CMOM CMNM

3

3.1

3-1 CMOM CMNM 3-1

3-1 CMOM CMNM S_0 S_1 S_0 S_1

CMNM 2 1

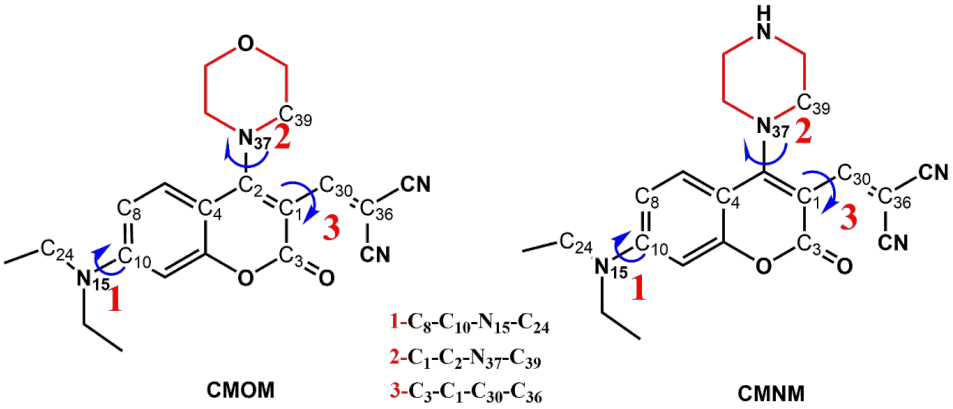
3 CMOM

2 1

3 3-1 3-1 CMNM CMOM

2 1

3



3-1

CMOM S0 S1 S0 S1 (C8-C18-N15-C24) (C3-C1-C30-C36) 6.69° 15.55° C1-C2-N37-C39

1 1-

CMOM S_0 S_1 S_0 S_1 (C_8-C_{18}-N_{15}-C_{24}) (C_3-C_1-C_{30}-C_{36}) 6.69° 15.55° C_1-C_2-N_{37}-C_{39}

1 1-

3-1 CMNM CMOM ° S_0 /S_1 Δ S_0 /S_1

		S_0	S_1	Δ
CMNM	1(C_8-C_{10}-N_{15}-C_{24})	-9.26	-2.11	7.15
	2(C_1-C_2-N_{37}-C_{39})	40.13	39.17	0.96
	3(C_3-C_1-C_{30}-C_{36})	31.33	45.91	14.58
CMOM	1(C_8-C_{10}-N_{15}-C_{24})	-9.10	-2.41	6.69
	2(C_1-C_2-N_{37}-C_{39})	40.67	38.96	1.71
	3(C_3-C_1-C_{30}-C_{36})	31.48	47.03	15.55

3.2

CMOM CMNM PCM DMSO

/ B3LYP/6-31G(d)

3-1 DMSO CMOM CMNM ΔE_{vert}

f HOMO→LUMO DMSO CMOM CMNM

CMOM CMOM 0.12 eV,CMOM 0.07 eV CMOM

0.97. 0.94 CMNM 0.95 0.94

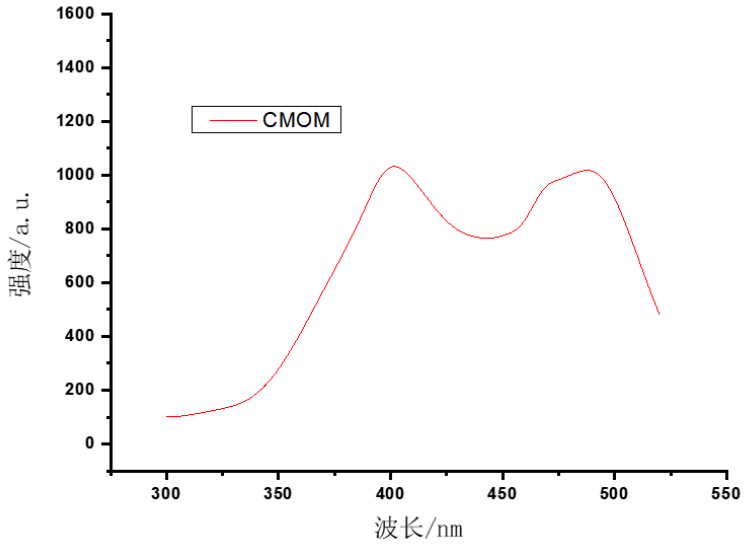
CMOM CMNM CMOM CMNM DMSO

3-1 DMSO CMOM CMNM ΔEvert f HOMO→LUMO DMSO CMOM CMNM CMOM CMOM 0.12 eV,CMOM 0.07 eV CMOM 0.97. 0.94 CMNM 0.95 0.94 CMOM CMNM CMOM CMNM DMSO CMOM CMOM CMOM CMNM CMOM CMNM HOMO→LUMO 98.80% 98%

CMOM CMOM CMOM CMNM CMOM CMNM HOMO→LUMO 98.80% 98%

3-2 DMSO CMOM CMNM ΔEvert Abs. Emi. *f* HOMO→LUMO

		ΔE_{vert}	Exp.	*f*	HOMO→LUMO
CMOM	Abs.	2.82 eV (439 nm)	2.70 eV (460 nm)	0.97	99.27%
	Emi.	2.34 eV (530 nm)	2.21 eV (560 nm)	0.94	98.83%
CMNM	Abs.	2.84 eV (437 nm)	N.A.	0.95	99.26%
	Emi.	2.36 eV (525 nm)	N.A.	0.94	98.91%



3-2 CMOM

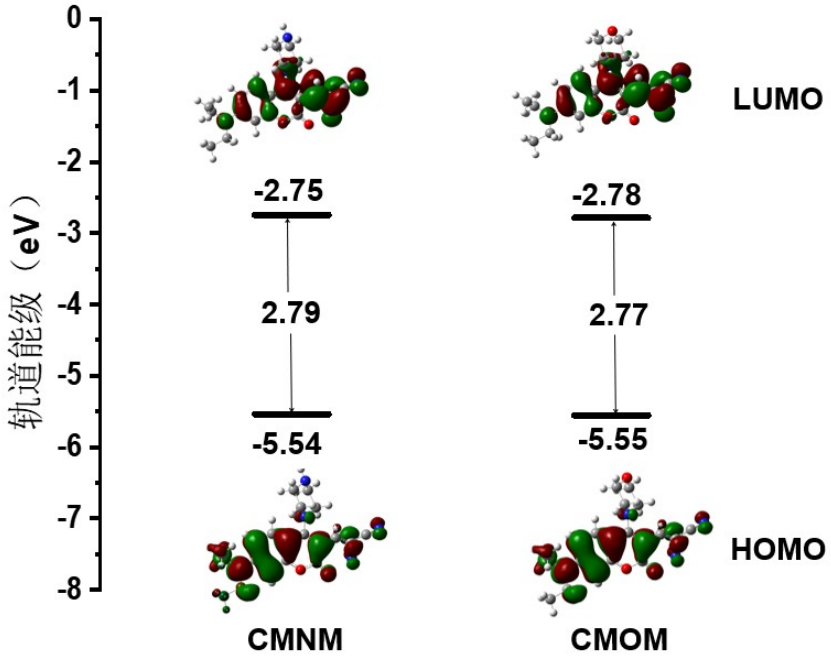
3-2 CMNM CMOM DMSO HOMO LUMO

HOMO→LUMO CMNM HOMO

LUMO HOMO

CMOM HOMO LUMO

HOMO



3-2 CMNM CMOM HUMO LUMO

3.3

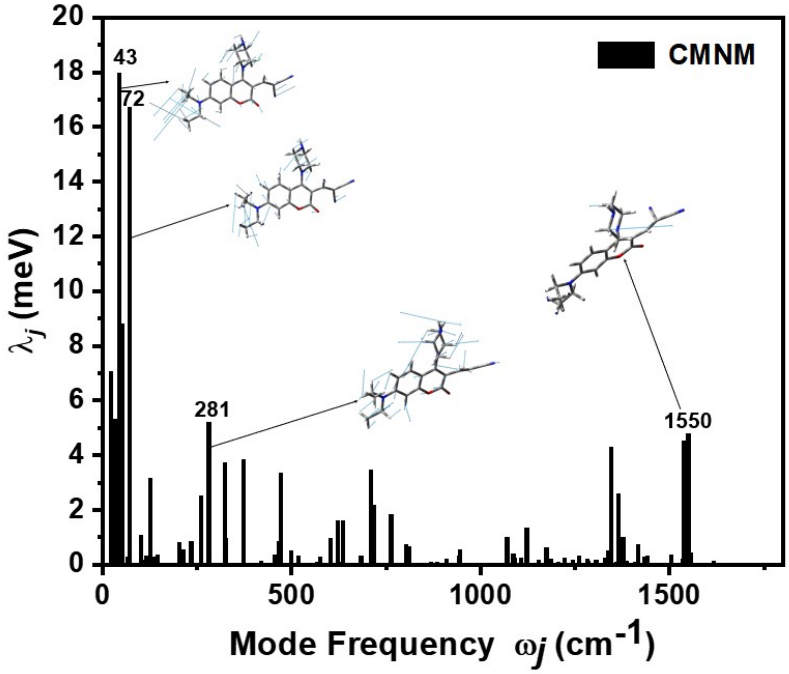
3-3 3-4 CMNM CMOM 3-3 3-4

CMNM CMOM

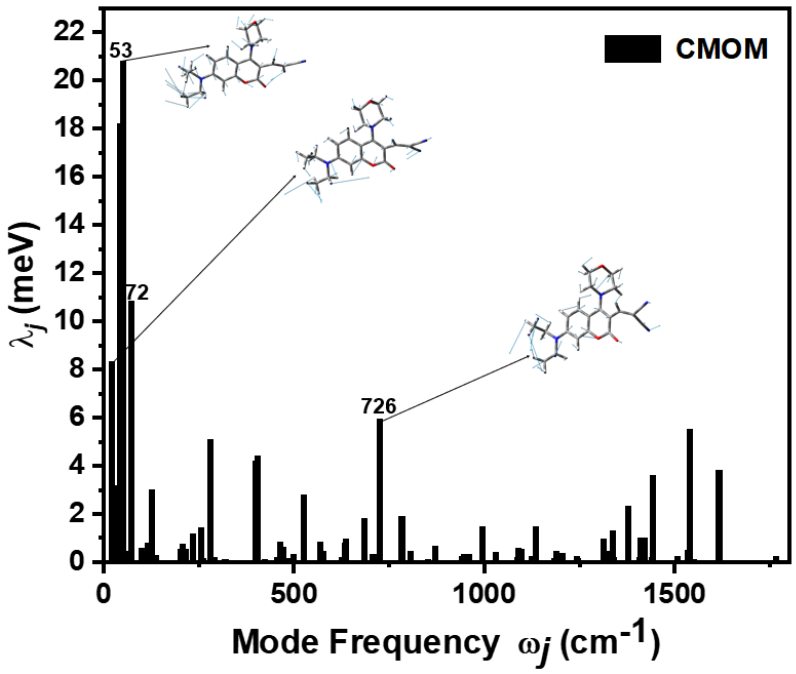
3-3 CMNM 43 cm^{-1} 72 cm^{-1} 281 cm^{-1}

1550 cm^{-1} CMOM 53 cm^{-1} 72

cm^{-1} 726 cm^{-1}



3-3 CMNM



3-4 CMOM

CMNM CMOM

3-5 3-5 CMNM

94% 6% CMOM

95% 5%

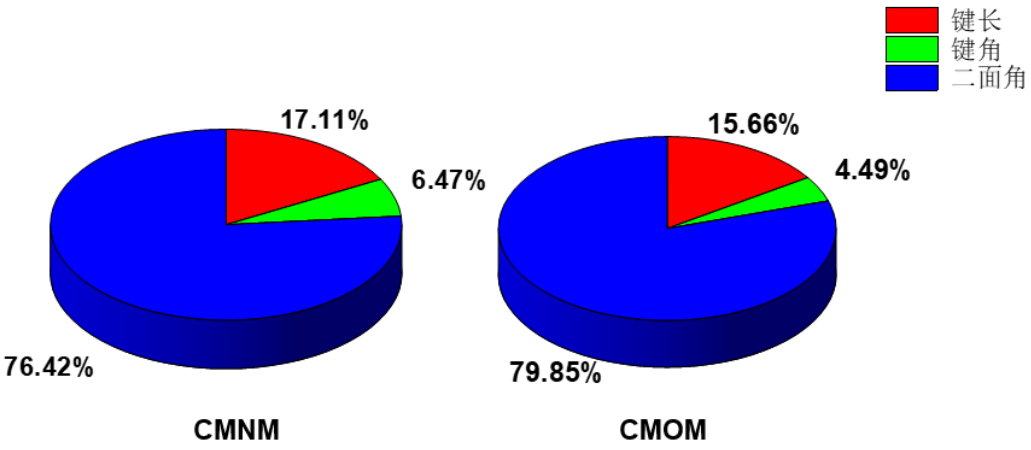
3-3 3-4 3-5

3-3 CMNM CMOM

λ_i 3-4 3-5 CMNM CMOM λ_i>1 meV

3-3 CMNM CMOM λ_i

CMNM	λ_i (meV)	30.88	11.68	137.95	180.51
CMOM	λ_i (meV)	29.80	8.56	111.15	149.51



3-5

3-4 CMNM λ_i>1 meV

Internal coordinates	λ_i (meV)	Internal coordinates	λ_i (meV)
B(C36-C30)	17.08	D(C3-C1-C30-C36)	9.99
B(C4-C2)	3.03	D(C2-N37-C38-H40)	7.62
B(C36-C32)	2.22	D(C2-C1-C30-H31)	4.32
B(C36-C33)	2.08	D(C2-N37-C38-C42)	3.48
B(N37-C2)	1.73	D(C2-N37-C38-H41)	3.44
B(C3-C1)	1.59	D(H31-C30-C36-	2.29

D(H31-C30-C36-C32)			
		C32)	
B(N34-C32)	1.41	D(C2-N37-C39-C45)	2.29
B(N35-C33)	1.36	D(H31-C30-C36-C33)	2.12
A(N35-C33-C36)	2.51	D(C2-N37-C39-H44)	1.98
A(C1-C2-N37)	2.34	D(N37-C2-C4-C6)	1.92
A(C4-C2-N37)	1.78	D(C3-C1-C30-H31)	1.91
A(C2-N37-C39)	1.22	D(C2-N37-C39-H43)	1.78
A(N37-C38-H41)	1.10	D(C24-N15-C27-H28)	1.67
D(C32-N34-C36-C33)	19.61	D(C3-C1-C2-N37)	1.55
D(C32-N34-C36-C30)	19.58	D(N37-C2-C4-C5)	1.38
D(C4-C2-N37-C38)	15.91	D(C30-C1-C3-O4)	1.34
D(C2-C1-C30-C36)	15.47	D(C8-C10-N15-C24)	1.17

D(C1-C2-N37-C38)			
D(C1-C2-N37-C38)	10.39		

3-5 CMOM $_i$>1 meV

Internal coordinates	λ_i (meV)	internal coordinates	λ_i (meV)
B(C36-C30)	16.55	D(C2-N37-C38-H41)	6.56
B(C4-C2)	3.60	D(C2-N37-C39-C45)	3.85
B(C36-C32)	2.18	D(C2-C1-C30-H31)	3.76
B(C36-C33)	2.02	D(C2-N37-C39-H43)	3.10
B(C3-C1)	1.58	D(C2-N37-C39-H44)	2.76
B(N34-C32)	1.37	D(N37-C2-C4-C6)	2.10
B(N35-C33)	1.33	D(H31-C30-C36-C32)	2.05

B(N37-C2)			
B(N37-C2)	1.07	D(H31-C30-C36-C33)	1.61
A(N35-C33-C36)	2.96	D(C3-C1-C2-N37)	1.60
A(C2-N37-C39)	1.70	D(C24-N15-C27-H28)	1.55
A(N37-C38-H41)	1.20	D(N37-C2-C4-C5)	1.49
D(C32-N34-C36-C33)	20.48	D(C30-C1-C3-C4)	1.25
D(C4-C2-N37-C38)	16.63	D(C3-C1-C30-H31)	1.25
D(C2-C1-C30-C36)	15.03	D(C8-C10-N15-C24)	1.09
D(C2-N37-C38-H40)	11.70		
D(C1-C2-N37-C38)	10.58		
D(C3-C1-C30-C36)	9.31		
D(C2-N37-C38-C42)	7.83		

3.4

3-6 CMNM CMOM DMSO

CMOM

3-6 CMNM CMOM DMSO CMOM

1.7% CMNM

2.0%

1.7% CMNM 2.0%

CMNM CMOM CMNM CMOM

CMNM CMOM 0.3%

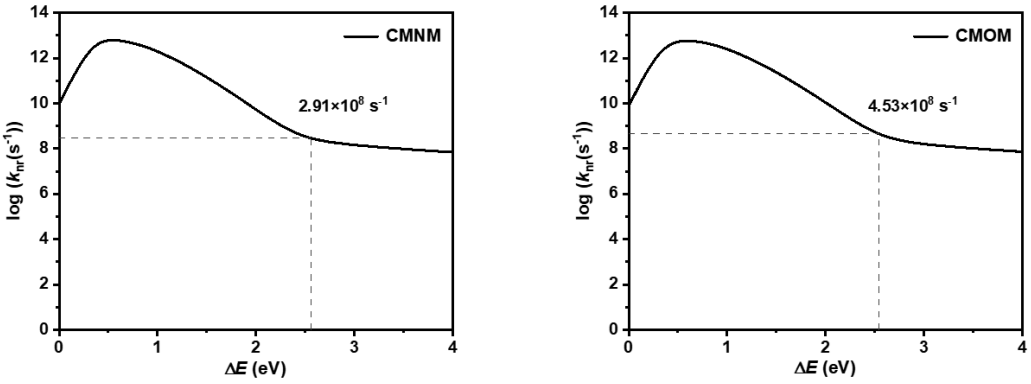
CMNM CMOM CMNM CMOM

CMNM CMOM

3-6 CMNM CMOM DMSO

	k_r	k_{ic}	Φ_f
CMNM	2.28×10^{8}	1.14×10^{10}	2.0%
CMOM	2.23×10^{8}	1.28×10^{10}	1.7%(1.3%)

, 3-6 $\log(k_c)\triangle E$ E k_c E $k\triangle E$ $\log(k)\triangle E$ 3-7 CMNM CMOM $\log(k_{ic})$ CMOM CMNM $\triangle E$



3-5 CMNM CMOM

PCM

CMOM CMNM

CMOM CMNM

1 1-

HOMO→LUMO CMOM CMNM CMOM

CMNM CMOM CMNM

CMOM CMOM CMNM HOMO→LUMO

98.80% 98%

CMOM CMNM

PCM

CMOM CMNM DMSO CMOM

CMNM DMSO 8

CMOM CMNM

CMNM

CMOM CMNM CMOM CMNM CMOM

CMOM CMNM DMSO CMOM CMNM DMSO 8

CMOM CMNM

CMNM CMOM CMNM CMOM

CMNM CMOM

[1] Yaneva Z, Ivanova D, Nikolova N, et al. Organic dyes in contemporary medicinal chemistry and biomedicine. I. From the chromophore to the bioimaging/bioassay agent[J]. Biotechnology & Biotechnological Equipment, 2022, 36(1): 1-14.

[2] Ferreira ES, Hulme AN, McNab H, et al. The natural con-stituents of historical textile dyes.Chem Soc Rev.2004;33(6):329–336.

[3] Hosseinnezhad M, Ghahari M, Mobarhan G, et al. Towards low cost and green photovoltaic devices: Using natural photosensitizers and MoS2/Graphene oxide composite counter electrodes[J]. Optical Materials, 2023, 139: 113775.

[4] Zhang F, Luo Y, Song J, et al. Triphenylamine-based dyes for dye-sensitized solar cells[J]. Dyes and Pigments, 2009, 81(3): 224-230.

[5] Dong H Q, Wei T B, Ma X Q, et al. 1, 8-Naphthalimide-based fluorescent chemosensors: recent advances and perspectives[J]. Journal of Materials Chemistry C, 2020, 8(39): 13501-13529.

[6] Han D M, Song H J, Han C H, et al. Enhancement of the outdoor stability of dye-sensitized solar cells by a spectrum conversion layer with 1, 8-naphthalimide derivatives[J]. RSC Advances, 2015, 5(41): 32588-32593.

[7] Gawas P P, Pandurangan P, Rabiei M, et al. Significance of Zn Complex Concentration on Microstructure Evolution and Corrosion Behavior of Al/WS2[J]. Molecules, 2023, 28(21): 7290.

[8] Lin Y J, Chen J W, Hsiao P T, et al. Efficiency improvement of dye-sensitized solar cells by in situ fluorescence resonance energy transfer[J]. Journal of materials chemistry A, 2017, 5(19): 9081-9089.

[9] Wycisk V, Achazi K, Hirsch O, et al. Heterobifunctional dyes: highly fluorescent linkers based on cyanine dyes[J]. ChemistryOpen, 2017, 6(3): 437-446.

[10] Takamura K, Fischer H, Morrow N R. Physical properties of aqueous glycerol solutions[J]. Journal of Petroleum Science and Engineering, 2012, 98: 50-60.

CMOM CMNM DMSO CMOM CMNM

DMSO 8

CMOM CMNM

CMNM CMOM CMNM CMOM

CMNM CMOM

[11] Licha K, Resch-Genger U. Fluorescent reporters and optical probes[M]//Comprehensive biomedical physics. Elsevier, 2014: Chapter 4.08, 85-109.

[12] Shaki H, Gharanjig K, Rouhani S, et al. Synthesis and photophysical properties of some novel fluorescent dyes based on naphthalimide derivatives[J]. Journal of Photochemistry and Photobiology A: Chemistry, 2010, 216(1): 44-50.

[13] Bardajee G R, Li A Y, Haley J C, et al. The synthesis and spectroscopic properties of novel, functional fluorescent naphthalimide dyes[J]. Dyes and Pigments, 2008, 79(1): 24-32.

[14] SOLTANI P H R, KHOSRAVI A R, GHARANJIG K A D, et al. Synthesis and characterization of new fluorescent polymerizable dyes based on naphthalimide[J]. 2010.

[15] Kim K W, Kim G H, Kwon S H, et al. Synthesis and photophysical properties of blue-emitting fluorescence dyes derived from naphthalimide derivatives containing a diacetylene linkage group[J]. Dyes and Pigments, 2018, 158: 353-361.

[16] Levitus M, Negri R M, Aramendia P F. Rotational relaxation of carbocyanines. Comparative study with the isomerization dynamics[J]. The Journal of Physical Chemistry, 1995, 99(39): 14231-14239.

[17] Rullière C. Laser action and photoisomerisation of 3, 3′-diethyl oxadicarbocyanine iodide (DODCI): Influence of temperature and concentration[J]. Chemical Physics Letters, 1976, 43(2): 303-308.

[18] Sanchez-Galvez A, Hunt P, Robb M A, et al. Ultrafast radiationless deactivation of organic dyes: evidence for a two-state two-mode pathway in polymethine cyanines[J]. Journal of the American Chemical Society, 2000, 122(12): 2911-2924.

[19] Kwon K C, Pallerla S. Viscosity of glycerol and its aqueous solutions measured by a tank-tube viscometer[J]. Chemical Engineering Communications, 2000, 183(1): 71-97.

[20] Scaffardi L, Di Paolo R E, Duchowicz R. Simultaneous absorption and fluorescence analysis of the cyanine dye DOCI[J]. Journal of Photochemistry and Photobiology A: Chemistry, 1997, 107(1-3): 185-188.

CMOM CMNM DMSO CMOM CMNM

DMSO 8

CMOM CMNM

CMNM CMOM CMNM CMOM

CMNM CMOM

[21] Aramendia P F, Negri R M, Roman E S. Temperature dependence of fluorescence and photoisomerization in symmetric carbocyanines. Influence of medium viscosity and molecular structure[J]. The Journal of Physical Chemistry, 1994, 98(12): 3165-3173.

[22] Sczepan M, Rettig W, Bricks Y L, et al. Unsymmetric cyanines: chemical rigidization and photophysical properties[J]. Journal of Photochemistry and Photobiology A: Chemistry, 1999, 124(1-2): 75-84.

[23] Sanborn M E, Connolly B K, Gurunathan K, et al. Fluorescence properties and photophysics of the sulfoindocyanine Cy3 linked covalently to DNA[J]. The Journal of Physical Chemistry B, 2007, 111(37): 11064-11074.

[24] Tasior M, Kim D, Singha S, et al. π-Expanded coumarins: synthesis, optical properties and applications[J]. Journal of Materials Chemistry C, 2015, 3(7): 1421-1446.

[25] Yang Z, Cao J, He Y, et al. Macro-/micro-environment-sensitive chemosensing and biological imaging[J]. Chemical Society Reviews, 2014, 43(13): 4563-4601.

[26] Jones G, Griffin S F, Choi C Y, et al. Electron donor-acceptor quenching and photoinduced electron transfer for coumarin dyes[J]. The Journal of Organic Chemistry, 1984, 49(15): 2705-2708.

[27] Kim H M, Cho B R. Small-molecule two-photon probes for bioimaging applications[J]. Chemical reviews, 2015, 115(11): 5014-5055.

[28] Chen J, Liu W, Zhou B, et al. Coumarin-and rhodamine-fused deep red fluorescent dyes: synthesis, photophysical properties, and bioimaging in vitro[J]. The Journal of organic chemistry, 2013, 78(12): 6121-6130.

[29] Kim D, Sambasivan S, Nam H, et al. Reaction-based two-photon probes for in vitro analysis and cellular imaging of monoamine oxidase activity[J]. Chemical Communications, 2012, 48(54): 6833-6835.

[30] Chan J, Dodani S C, Chang C J. Reaction-based small-molecule fluorescent probes for chemoselective bioimaging[J]. Nature chemistry, 2012, 4(12): 973-984.

[31]McConnell G, Riis E. Two-photon laser scanning fluorescence microscopy using photonic crystal fiber[J]. Journal of biomedical optics, 2004, 9(5): 922-927.

[32]Zhang Z Q, Yao W J, Qiao L L, et al. A Lysosome-Targetable Fluorescence Probe Based on L-Cysteine-Polyamine-Morpholine-Modified Quantum Dots for Imaging in Living Cells[J]. International Journal of Nanomedicine, 2020: 1611-1622.

[33]Zhang J, Yang M, Li C, et al. Near-infrared fluorescent probes based on piperazine-functionalized BODIPY dyes for sensitive detection of lysosomal pH[J]. Journal of Materials Chemistry B, 2015, 3(10): 2173-2184.

[34]Yang J, Yu Y, Wang B, et al. A sensitive fluorescent probe based on coumarin for detection of cysteine in living cells[J]. Journal of Photochemistry and Photobiology A: Chemistry, 2017, 338: 178-182.

[35]Majhi A, Venkateswarlu K, Sasikumar P. Coumarin Based Fluorescent Probe for Detecting Heavy Metal Ions[J]. Journal of Fluorescence, 2023: 1-31.

[36]Sun X, Liu T, Sun J, et al. Synthesis and application of coumarin fluorescence probes[J]. RSC advances, 2020, 10(18): 10826-10847.

[37]Feit M D, Fleck Jr J A, Steiger A. Solution of the Schrödinger equation by a spectral method. J. Comput. Phys. 1982, 47: 412-433.

[38]Hosseinnejad T, Mahdavian S. Quantum chemistry study on regioselectivity in ruthenium catalyzed synthesis of 1, 5-disubstituted 1, 2, 3-triazoles. Comput. Theor. Chem. 2018, 1143: 29-35.

[39]Li J, Jiang Y B, Cheng J, et al. Tuning the singlet-triplet energy gap of AIE luminogens: crystallization-induced room temperature phosphorescence and delay fluorescence, tunable temperature response, highly efficient non-doped organic light-emitting diodes. Phys. Chem. Chem. Phys. 2015, 17: 1134-1141.

[40]Yang H L, Zhang Q P, Zhang Y M, et al. A novel strong AIE bi-component hydrogel as a multi-functional supramolecular fluorescent material. Dyes Pigm. 2019, 171: 107745.

[41]Suresh R, Thiyagarajan S K, Ramamurthy P. An AIE based fluorescent probe for digital lifting of latent fingerprint marks down to minutiae level. Sensor. Actuat. B-Chem. 2018, 258: 184-192.